JOURNAL OF CATALYSIS **161,** 222–229 (1996)
ARTICLE NO. 0180

Light Naphtha Isomerization over Mordenite-Supported Ni–Pt Catalysts: Effects of Ni on the Catalytic Performance for Pure Feed and Sulfur-Containing Feed

R.-M. Jao,* T.-B. Lin,† and J.-R. Chang*,[1]

*Department of Chemical Engineering, National Chung Cheng University; and †Refining & Manufacturing Research Center, Chinese Petroleum Corporation, Chia-Yi, Taiwan, Republic of China

Received August 25, 1995; revised February 6, 1996; accepted February 12, 1996

Temperature-programmed reduction (TPR) and temperature programmed desorption (TPD) of NH_3 were used to characterize bimetallic interactions and the acidity of mordenite-supported Pt and Ni–Pt catalysts. The effects of adding Ni to the Pt catalysts were investigated by examining (1) total conversion, fuel gas formation, and rate of branched isomer formation of pure C_5 (*n*-pentane), C_6 (*n*-hexane), and C_7 (*n*-hexane) reactions catalyzed by the Pt and Ni–Pt catalysts; and (2) the stability of the catalysts with C_6 feed containing 500 ppm sulfur. The test reactions were carried out under operating conditions similar to those of a commercial isomerization process. For pure feed, the reaction results indicated that addition of a moderate amount of Ni to the Pt catalyst not only suppresses fuel gas formation, but facilitates the formation of branched isomers. However, for sulfur-containing feed, no suppression of fuel gas formation was observed. Instead, the Ni–Pt catalyst underwent a more rapid deactivation and produced more fuel gas than did the Pt catalyst. Together with the catalytic performance test and the TPD and TPR results, the relatively high catalyst deactivation and fuel gas formation rate are associated with the poor sulfur resistance of the catalyst caused by Ni–Pt bimetallic interactions. © 1996 Academic Press, Inc.

INTRODUCTION

Light naphtha isomerization processes normally use high-activity chlorided alumina or bifunctional zeolite catalysts to convert *n*-pentane and *n*-hexane to more highly branched isomers of higher octane number (1). High-activity chlorided catalysts [$Pt/Al_2O_3(Cl)$] consist of a metal and a support, generally platinum/alumina, and their acidity is increased by halogenation (Cl, F) of the base (1). In contrast to bifunctional zeolite catalysts, these catalysts are relatively active, allowing the process to operate at lower temperature. Since the isomerization reaction is slightly exothermic ($\Delta H = -4$ to -20 kJ/mol), from a thermodynamical point of view, low temperatures favor the production of the isomers with a high octane lavel. However, these catalysts are very sensitive to poisons such as water and sulfur compounds (2, 3). Moreover, corrosion caused by the injection of chloride into the feed for maintaining activity also brings difficulty in equipment maintenance.

Bifunctional zeolite catalysts have no corrosion problems and are less sensitive to sulfur and water. However, because of their low acidity, these catalysts have to be used at relatively high temperatures to form carbeniums for carrying out C_5/C_6 isomerization reactions. The necessary high-temperature operation promotes the C_7^+ (compounds, contained in light naphtha, with molecular weight greater than or equal to that of heptane) hydrocracking rate and, thus, leads to the formation of fuel gas and coke (4).

Bimetallic catalysts have been proved to have potential in fine-tuning the selectivity of heterogeneous catalysts, and have already been exploited in petroleum refining processes (5–8). This study reports the role of Ni in light naphtha isomerization catalyzed by Ni–Pt/mordenite catalysts. Nickel was chosen as the second metal to modify the catalytic properties of the Pt catalyst, because (i) reports of alloy formation between Ni and Pt, along with a common fcc (face-centered cubic) lattice structures (9, 10), suggest the potential for bimetallic interactions between two metals, and (ii) by the addition of Ni to Pt/mordenite catalysts, the metallic-to-acid-sites ratio may be increased, thereby increasing the C_7^+ tolerance of the Pt catalysts.

The test reactions were carried out at a total pressure of 29 atm, weight hourly space velocity (WHSV) of 1.4 (g of feed/h/g of catalyst), and temperatures ranging from 220 to 290°C; the operation conditions are similar to those in commercial plants (1, 2). C_5 and C_6 isomerization were used as model reactions to examine the rate of branched isomer formation catalyzed by the catalysts, and C_7 was chosen as a feed to examine hydrocracking selectivity. Catalytic performance of the catalysts for sulfur-containing feed was also tested because isomerization activity is decreased with sulfur-bearing feeds, and about half of the refineries worldwide do not hydrodesulfurize the C_5/C_6 fraction of the gasoline pool (2). Thiophene was used as the model sulfur

[1] To whom correspondence should be addressed.

0021-9517/96 $18.00

compound and C_6 containing 500 ppm sulfur was used as a feed for the tests.

EXPERIMENTAL

Materials and Catalyst Preparation

Mordenite zeolite was supplied by Conteka with a Si/Al atomic ratio of 14 and 0.3 wt% Na_2O. The zeolite (30 g) was treated with 200 ml of an aqueous solution of $Pt(NH_3)_4Cl_2$ (Strem, used without purification) containing an amount of Pt that would have yielded a solid containing 0.3 wt% Pt, provided that all the Pt had been taken up by zeolite. The pH of the solution was held at 8.0 by adding 1 *N* NH_4OH and the zeolite slurry was stirred at 80°C for 12 h to perform ion exchange. The sample was then filtered and the recovered solid was washed with distilled water and dried in air at room temperature for 8 h. The filtrate was mixed with the resulting solid, and the slurry was stirred again. This ion-exchange cycle was repeated three times and followed with drying at 120°C for 4 h and calcination at 450°C in flowing dry air at atmospheric pressure for 6 h. The resultant catalyst contained 0.26 wt% Pt (determined by inductively coupled plasma optical emission spectroscopy with a Jarnell-Ash 110 instrument). This catalyst sample was noted as Pt(0.26). Part of this Pt catalyst sample was treated with $Ni(NO_3)_2 \cdot 6H_2O$(Aldrich) aqueous solution to make Ni–Pt catalyst samples. They were prepared by incipient wetness impregnation method with just enough solution to give 0.5 and 1.5 wt% Ni content. After the impregnation, the catalyst sample was dried at 120°C for 12 h, and calcined at 450°C for 4 h. These two Ni–Pt catalyst samples were noted as Ni(0.5)–Pt(0.26) and Ni(1.5)–Pt(0.26), respectively.

Catalytic Performance Test

The catalytic performance tests were carried out with a continuous-downflow fixed-bed reactor. The reactor was a stainless-steel tube with an inside diameter of 1.1 cm. It was heated electrically and the temperature controlled by a PID temperature controller with a sensor at the outer wall of the reactor. The temperature difference between the outer reactor wall and the center of the catalyst bed was about 10°C. The reactor was packed with 2.0 g of catalyst particle size 1000–2000 μm. The ratio of bed length to catalyst particle diameter was approximately 65; the axial dispersion effects are inferred to have been negligible. The upstream part of the reactor was a preheated zone filled with particles of a catalytically inactive ceramic material.

The reaction system was first purged with dry nitrogen gas for 4 h to remove residual hydrocarbons. The catalysts were then reduced at 450°C under 29 atm pure hydrogen for 4 h. After reduction, the catalytic reactions were carried out with a WHSV of 1.4 (g of feed/h/g of catalyst), at 220 to 290°C and 29 atm. Liquid products were trapped by condenser at −5°C. Samples were collected periodically and analyzed by gas chromatography. Before the reaction, the feeds, *n*-pentane, *n*-hexane, and *n*-heptane (Aldrich), were dried with particles of activated 4-Å molecular sieve. Ninety-eight percent (±2%) of the feed was recovered as reaction products, as estimated by material balance calculations. The 2% loss is attributed to hydrocarbons deposited on the walls of the reaction system, on the catalyst, and on the surface of ceramic reactor packing.

To investigate the role of Ni on the catalytic performance with feed containing sulfur, thiophene was added to C_6 to prepare a feed of 500 ppm sulfur content. To prevent any sulfur contamination, before reaction, the reaction system was purged with dried air for 8 h a 600°C. Catalyst samples were reduced in flowing hydrogen at 29 atm. After reduction, the temperature was lowered to the reaction temperature. The catalytic reactions were carried out with a WHSV of 2.5 and an H_2-to-oil mole ratio of 4.7, at 250°C under 29 atm.

The GC system used for feed and reacted sample analysis was a Shimadzu Model GC-14B gas chromatograph equipped with a SGE fused silica capillary column of 50 m × 0.15 mm i.d. (50QC1.5/BP1 PONA) and flame ionization detector. The column was operated at 35°C for 15 min, then to 110°C at 5°C/min with linear velocity 20 cm/min dry nitrogen.

Catalyst Characterization

Temperature-programmed reduction. The apparatus used for the temperature-programmed reduction (TPR) and temperature programmed desorption (TPD) was described by Jones and McNicol (11). A gas stream of 10% H_2 in argon passed through the catalyst sample (0.5 g) in a quartz reactor heated at 10°C/min to 800°C with a temperature-programmed furnace. The water produced by reduction was trapped into a column of silica gel. The amount of H_2 consumption was detected with a thermal conductivity detector (TCD). The reduction temperature was monitored by a k-type thermocouple.

Temperature-programmed desorption. A quartz tube was packed with a small amount (0.3 g) of catalyst sample. The catalyst sample was then reduced under the same operating conditions used in the catalytic performance test except at 1 atm. After the reduction, the sample was further dried in flowing He at 500°C for 4 h and then cooled to room temperature. When the system become steady (20 ml/min He flow rate and 40°C), 1 ml NH_3 was injected onto catalyst bed through He carrier gas. The injections were repeating until none of chemisorbed NH_3 was detected with the TCD. Desorption experiments were then carried out with He flowing at 20 ml/min He at 1 atm by increasing catalyst bed temperature from 40 to 700°C at 20°C/min. Evolved NH_3 was again monitored with the TCD.

CO chemisorption. About 1.0 g catalyst was packed in a stainless-steel tube and then reduced under the same operating conditions used in the catalytic performance test. After the reduction, the tube was hooked up to a Shimadzu Model GC-14B gas chromatograph with a TCD. The tube for adsorption measurement was connected to a three-way ball valve and the connection ports were carefully purged with He before switching gas flow to the catalyst bed to inhibit any air contamination. After the system become steady (20 ml/min He flow rate and 35°C), a 0.1-ml pulse of CO was repeatedly injected into the catalyst bed with He carrier gas until none of the pulse was chemisorbed. The amount of chemisorption was then calculated by summing up the proportions of all pulses consumed.

RESULTS

Temperature-Programmed Desorption

The TPD profiles characterizing NH_3 adsorbed on Pt and Ni–Pt catalysts are shown in Fig. 1. No significant TPD peaks are observed for the blank test sample (the mordenite-supported Pt catalyst without any NH_3 adsorption). The Pt catalyst sample and the Ni–Pt catalyst samples exhibit two maxima in the rate of NH_3 desorption at about 290°C and about 540°C. Peak position did not vary substantially with the increase in metal loading. Whereas the amount NH_3 adsorbed on the catalyst decreases with increasing metal loading: 2.68 mmol/g for the Pt(0.26) catalyst, 2.36 mmol/g for the Ni(0.5)–Pt(0.26) catalyst, and 1.76 mmol/g for the Ni(1.5)–Pt(0.26) catalyst.

Temperature-Programmed Reduction

As shown in Fig. 2, the maximum reduction rate of the mordenite-supported Ni catalyst is at 480°C, and that of the Pt catalyst, at 260°C. The reduction temperature of Ni–Pt catalyst samples decreased with the increase in Pt concentration: the maximum reduction rate is at 345°C for Ni(0.5)–Pt(0.26) catalyst and at 380°C for Ni(1.5)–Pt(0.26) catalyst. Moreover, Ni(0.5)–Pt(0.26) catalysts are characterized by a single peak. In contrast, the TPR of a physical mixture of the Ni catalyst and the Pt catalyst showed maxima in reduction rate similar to those of the summation the TPR spectra characterizing the single Pt and single Ni catalyst.

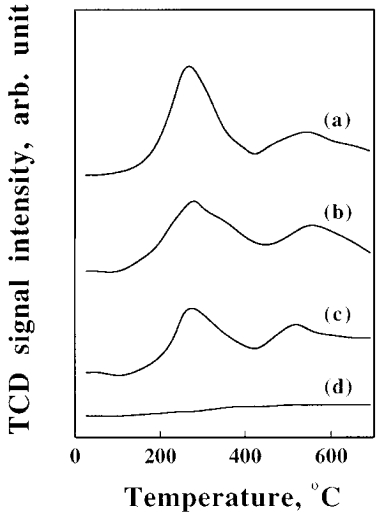

FIG. 1. NH_3 TPD profiles for (a) Pt(0.26), (b) Ni(0.5)–Pt(0.26), (c) Ni(1.5)–Pt(0.26), and (d) bland test [Pt(0.26) without NH_3 adsorption].

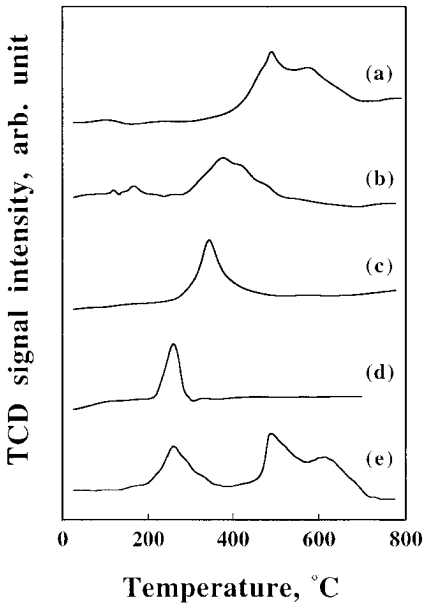

FIG. 2. TPR profiles for (a) mordenite-supported Ni catalyst, (b) Ni(1.5)–Pt(0.26), (c) Ni(0.5)–Pt(0.26), (d) Pt(0.26), and (e) mixture of mordenite-supported Ni catalyst and Pt(0.26) catalyst.

Catalytic Performance Test

The catalytic conversion of light naphtha is greatly influenced by reaction temperature. As shown in Figs. 3 and 4, C_7 reaction rate (μmol n-C_n reacted/s/g of catalyst) and fuel gas (C_1–C_4) formation [(g of fuel gas formed)/(g of n-C_n feed) × 100] increased with increasing reaction temperature, whereas the rate of branched isomer formation (μmol of C_n branched isomer formed/s/g of catalyst) exhibited a maximum at about 250°C (Fig. 5). The addition of Ni to the Pt catalyst inhibits both the total conversion of C_7 and fuel gas formation (Figs. 3 and 4), while among the three catalyst samples, the Ni(0.5)–Pt(0.26) catalyst presents the highest branched isomer formation rate (Fig. 5). The C_7 catalytic reaction results are summarized in Table 1.

As shown in Figs. 6 and 7, for pure C_6 feed, total conversion and fuel gas formation increased with increasing reaction temperature, similar to the C_7 catalytic reactions. However, since the fuel gas formed from C_6 reaction is much lower than that formed from C_7, within the reaction temperature range (220–290°C), the branched isomer

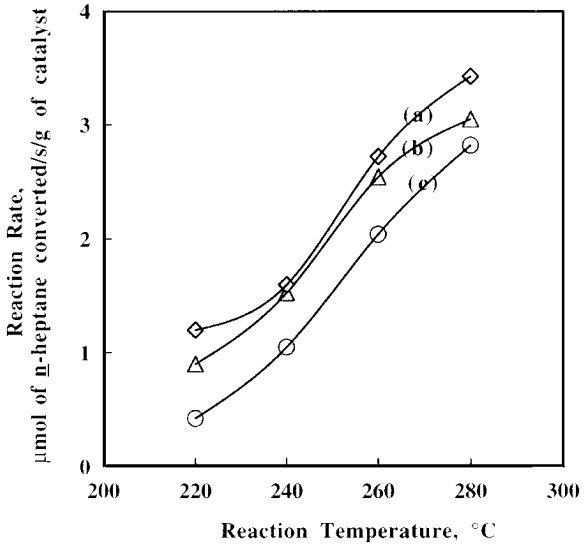

FIG. 3. Total conversion of pure *n*-heptane catalyzed by (a) ◇, Pt(0.26) catalyst; (b) △, Ni(0.5)–Pt(0.26) catalyst; and (c) ○, Ni(1.5)–Pt(0.26) catalyst.

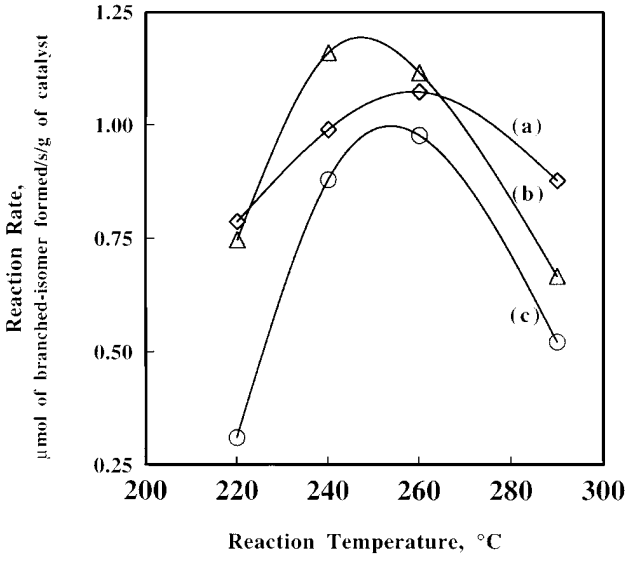

FIG. 5. Rate of branched isomer formation for pure *n*-heptane feed catalyzed by (a) ◇, Pt(0.26) catalyst; (b) △, Ni(0.5)–Pt(0.26) catalyst; and (c) ○, Ni(1.5)–Pt(0.26) catalyst.

formation rate also increases with elevating reaction temperature (Fig. 8).

For pure C_6 feed, the Ni(0.5)–Pt(0.26) catalyst presents the highest conversion and the highest branched isomer formation rate of the three catalyst samples. The C_6 catalytic reaction results are summarized in Table 2. The effects of the addition of Ni and reaction temperature on the branched isomer formation rate of C_5 are the same as those on C_6 and the results are shown in Fig. 9.

For the C_6 feed containing 500 ppm sulfur, fuel gas formation and total conversion as a function of time on stream are shown in Figs. 10 and 11, respectively, for Pt(0.26) catalyst and Ni(0.5)–Pt(0.26) catalyst. The total conversion and fuel gas formation of the Ni(0.5)–Pt(0.26) catalyst were higher than those of the Pt(0.26) catalyst at the start of run, but they also fell more rapidly than those of the Pt(0.26) catalyst. However, as shown in Fig. 12, thiophene conversion

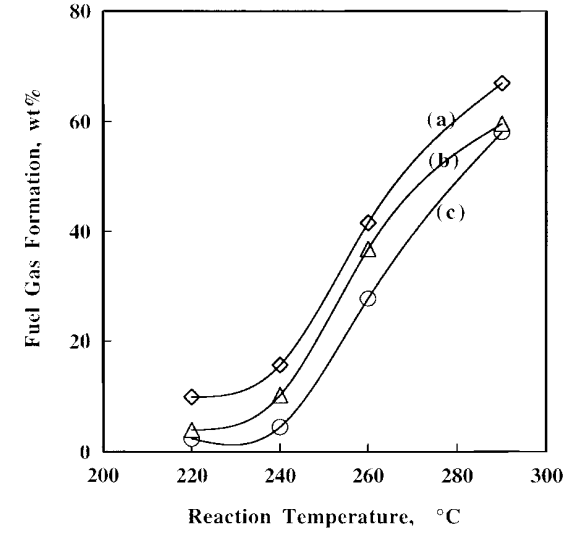

FIG. 4. Fuel gas formation of pure *n*-heptane catalyzed by (a) ◇, Pt(0.26) catalyst; (b) △, Ni(0.5)–Pt(0.26) catalyst; and (c) ○, Ni(1.5)–Pt(0.26) catalyst.

TABLE 1

Summary of *n*-Heptane Reaction with WHSV = 1.4 h^{-1} and H_2/Oil = 4.7 at 410 psig and 240°C Catalyzed by Mordenite-Supported Pt and Ni–Pt Catalysts

Product distribution (wt%)	Pt (0.26)	Ni(0.5)–Pt(0.26)	Ni(1.5)–Pt(0.26)
C_1–C_3	11.10	4.67	1.91
i-C_4	4.20	4.25	2.43
n-C_4	0.26	0.46	0.10
i-C_5	0.10	0.73	0.17
n-C_5	0.02	0.25	0.10
i-C_6	0.11	0.43	0.07
n-C_6	0.04	0.22	0.04
$22DMC_5$	1.25	1.44	0.65
$24DMC_5$	2.04	1.91	1.91
$223TMC_4$	0.20	0.21	0.13
$33DMC_5$	0.49	0.55	0.26
$2MC_6$	9.01	10.59	8.04
$23DMC_5$	2.60	2.75	2.30
$3MC_6$	8.72	9.50	8.38
$3EC_5$	0.94	1.31	0.50
n-C_7	58.92	60.73	73.00
Conversion (wt%)	41.08	39.27	27.00
Fuel gas (wt%)	15.56	9.38	4.44
Rate of branched isomer formation (μmol/s/g)	0.99	1.16	0.87

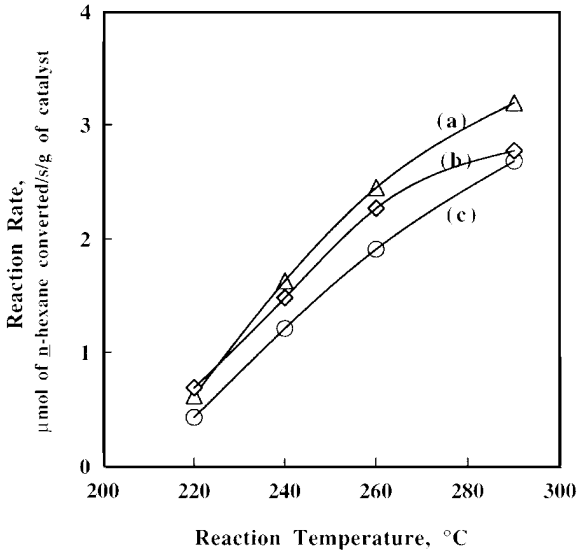

FIG. 6. Total conversion of pure *n*-hexane catalyzed by (a) △, Ni(0.5)–Pt(0.26) catalyst; (b) ◇, Pt(0.26) catalyst; and (c) ○, Ni(1.5)–Pt(0.26) catalyst.

TABLE 2

Summary of *n*-Hexane Reaction with WHSV = 1.4 h^{-1} and H_2/Oil = 4.7 at 410 psig and 240°C Catalyzed by Mordenite-Supported Pt and Ni–Pt Catalysts

Product distribution (wt%)	Pt(0.26)	Ni(0.5)–Pt(0.26)	Ni(1.5)–Pt(0.26)
C_1–C_3	0.18	0.24	0.03
i-C_4	0.22	0.15	0.09
n-C_4	0.09	0.01	0.01
i-C_5	0.99	0.87	0.51
n-C_5	0.46	0.53	0.04
$22DMC_4$	1.57	2.02	0.96
$23DMC_4$	1.88	2.21	1.15
$2MC_5$	17.44	18.62	15.57
$3MC_5$	10.46	11.44	8.40
n-C_6	66.71	63.91	73.24
Conversion (wt%)	33.29	36.09	26.76
Fuel gas (wt%)	0.49	0.40	0.13
Rate of branched isomer formation (μmol/s/g)	1.47	1.60	1.21

increased with time on stream and became time invariant after 10 h. In the near steady state, the thiophene conversion of the Pt(0.26) catalyst is higher than that of the Ni(0.5)–Pt(0.26) catalyst.

DISCUSSION

The acidity and Ni–Pt bimetallic interactions of the catalysts investigated in this study have been characterized by NH_3 TPD and TPR, respectively. These catalysts were also tested both in the presence and in the absence of sulfur in catalytic reactions representative of light naphtha isomerization. Together with the characterization and performance test data, the role of Ni in affecting the catalytic properties was elucidated.

Acidity of the Supported Pt and Ni–Pt Catalysts

The acidity of the mordenite-supported Pt and Ni–Pt catalysts was characterized by TPD of the ammonium form of the mordenite support, and the results are shown in Fig. 1.

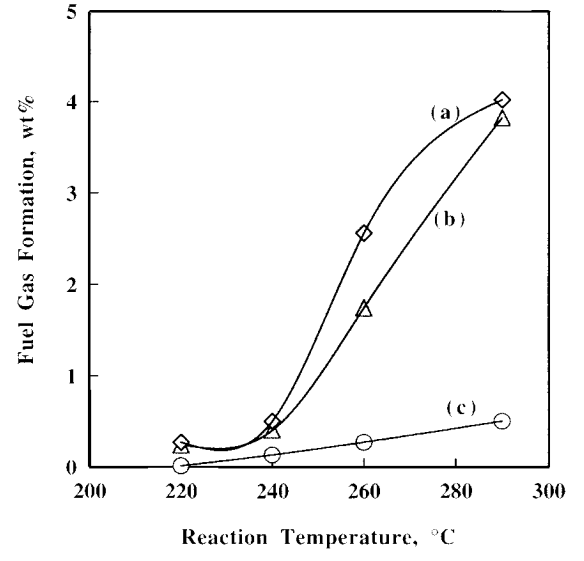

FIG. 7. Fuel gas formation of pure *n*-hexane catalyzed by (a) ◇, Pt(0.26) catalyst; (b) △, Ni(0.5)–Pt(0.26) catalyst; and (c) ○, Ni(1.5)–Pt(0.26) catalyst.

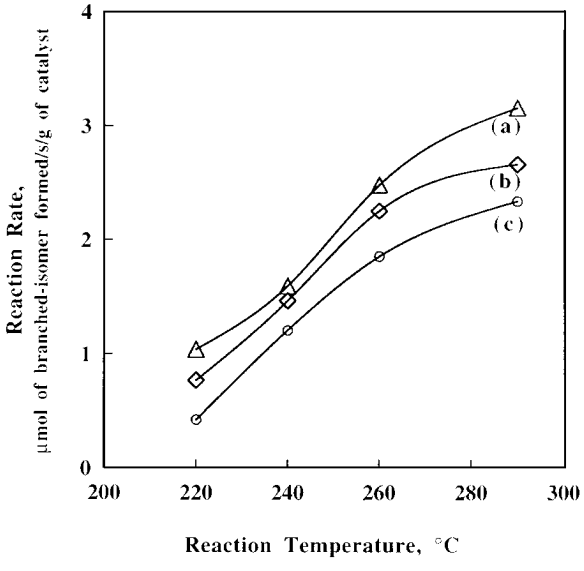

FIG. 8. Rate of branched isomer formation for pure *n*-hexane feed catalyzed by (a) △, Ni(0.5)–Pt(0.26) catalyst; (b) ◇, Pt(0.26) catalyst; and (c) ○, Ni(1.5)–Pt(0.26) catalyst.

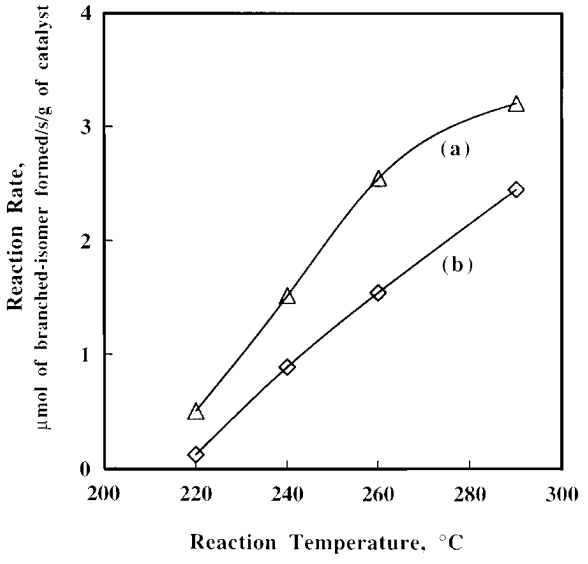

FIG. 9. Rate of branched isomer formation for pure *n*-pentane feed catalyzed by (a) △, Ni(0.5)–Pt(0.26) catalyst and (b) ◇, Pt(0.26) catalyst.

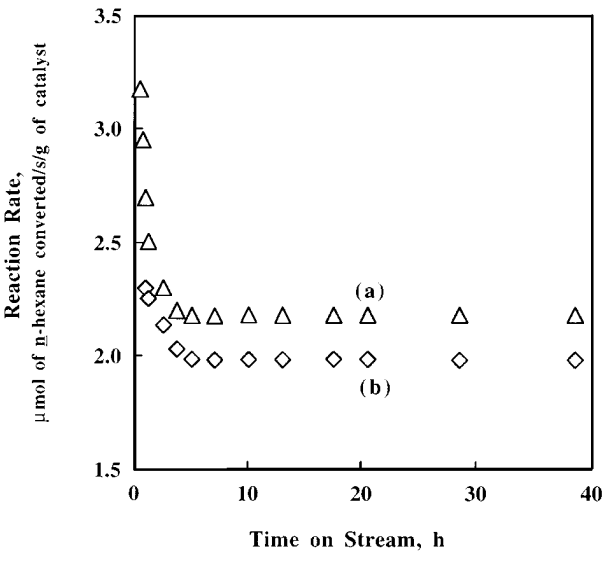

FIG. 11. Total conversion of *n*-hexane feed containing 500 ppm sulfur catalyzed by (a) △, Ni(0.5)–Pt(0.26) catalyst and (b) ◇, Pt(0.26) catalyst.

No significant TPD peaks were observed for the blank test sample. In contrast, two peaks, one at about 290°C and one at about 540°C, were observed for the Pt and Ni–Pt catalyst samples. Since the ammonia desorption temperature and the amount of ammonia evolved are considered respectively as indexes of acid strength and of acid amount (12), comparison of the NH_3 TPD chromatograms of the Pt and Ni–Pt catalyst samples allows us to investigate the effects of metal addition to the catalysts on catalyst acidity. As indicated in Fig. 1, among the three catalyst samples, no significant change in the TPD peak position was observed. This result suggests the acid strength of the catalysts did not vary with metal addition. However, a decrease in peak area with the increase in metal loading was observed. The decrease in peak area suggests that the acid sites were partially covered by the deposited metal particles and the acid amount of the catalyst decreased with increasing metal loading.

Temperature-Programmed Reduction of the Supported Pt and Ni–Pt Catalysts

As shown in Fig. 2, the reduction temperature of the Ni–Pt catalyst samples decreased with increasing Pt concentra-

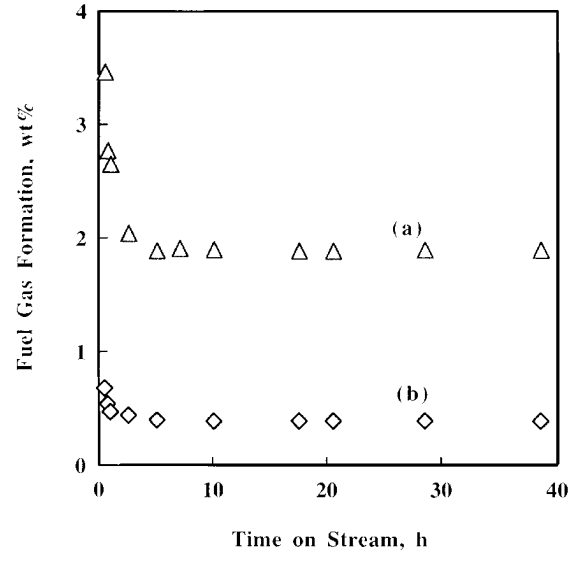

FIG. 10. Fuel gas formation of *n*-hexane feed containing 500 ppm sulfur catalyzed by (a) △, Ni(0.5)–Pt(0.26) catalyst and (b) ◇, Pt(0.26) catalyst.

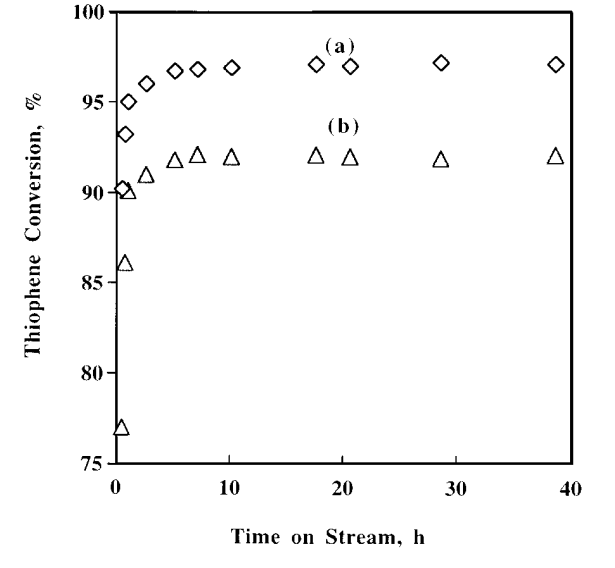

FIG. 12. Thiophene conversion of *n*-hexane feed containing 500 ppm sulfur catalyzed by (a) ◇, Pt(0.26) catalyst and (b) △, Ni(0.5)–Pt(0.26) catalyst.

tion of the catalysts and the Ni(0.5)–Pt(0.26) catalysts are characterized by a single peak. Similar results for TPR characterizing silica-supported Ni–Pt catalysts were reported by Raab *et al.* (13); they observed only a sharp maximum in the rate of reduction at 266°C for the Ni–Pt catalysts with Pt concentration greater than 50 mol%. TPR of physical mixtures of Ni and Pt catalyst samples however, showed that the Ni and Pt were reduced separately and the maximum reduction rate of Ni exhibited no significant change compared with that of the Ni catalyst alone.

Inferred from the mechanism for the platinum-catalyzed reduction of rhenium in PtRe/γ-Al_2O_3 (14), the decrease in Ni reduction temperature with increasing Pt concentration and the TPR spectra characterized by a single peak of the Ni(0.5)–Pt(0.26) catalyst may indicate a catalytic reduction of Ni. Presumably, mobile platinum oxide and/or nickel oxide particles collide into each other by thermal migration and the nickel oxide particles are catalytically reduced by prereduced Pt particles. This postulate suggests the formation of Ni–Pt bimetallic interactions. However, since TPR is not a conclusive technique to determine the formation of bimetallic interactions, the TPR spectrum characterizing the Ni–Pt catalysts can alternatively be explained by spillover of hydrogen from the reduced Pt to the nickel oxide via the alumina support (15). The difference in Ni reduction temperature between the Ni–Pt catalysts and the physical mixture of Ni and Pt catalyst samples is explained by the assumption that the Ni reduction temperature is determined by the rate of hydrogen transport from Pt to Ni. Increasing Pt concentration or decreasing hydrogen transport path decreases the reduction temperature of Ni. Based on this explanation, segregate Ni and Pt particles are expected to form on the alumina surface.

Catalytic Properties of Pt and Ni–Pt Catalysts for Pure C_5, C_6, and C_7

As shown in Figs. 3 and 4, C_7 reaction rate and the fuel gas formation decreased with the increase in Ni content and increased with reaction temperature. However, among these catalysts and operating conditions, the Ni(0.5)–Pt(0.26) catalyst runs at about 250°C produced the highest branched isomer formation rate (Fig. 5).

The catalytic properties of the Pt and Ni–Pt catalysts for pure feed can be explained by a bifunctional reaction mechanism. The decrease in fuel gas formation with increasing Ni content of the catalysts was thought to be caused by the increase in the metallic site/acid site ratio (N_M/N_A, where N_M is calculated from CO chemisorption and N_A is calculated from TPD of NH_3): the ratio is 0.0044 for the Pt(0.26) catalyst and 0.0059 for the Ni(0.5)–Pt(0.26) catalyst. For a catalyst with a higher metallic/acid sites ratio, the diffusion path between two metallic sites is shorter than for a catalyst with fewer metallic sites. Hence, the possibility that the olefinic intermediate would encounter acid sites and would be cracked during its migration from one metallic site to another is also lower. Similar results were reported by Guisnet *et al.* (16, 17). For C_7 reacted over Pt/HY catalysts, cracking rate decreased with the increase in Pt content up to 1 wt% and then became invariant with Pt loading.

Increased reaction temperature enhances C_7 and C_6 conversion, as shown in Figs. 3 and 6, but it also prompts fuel gas formation (Figs. 4 and 7). Thus, within the reaction temperature range (220–290°C) the highest branched isomer formation rate for C_7 was obtained at 250°C (Fig. 5), which is a compromise between conversion and fuel gas formation. However, since fuel gas formation for C_6 is much lower than that for C_7, the C_6 branched isomer formation rate increased with increasing reaction temperature (Fig. 8).

As indicated by CO chemisorption characterizing metal dispersion and TPD characterizing catalyst acidity, the addition of Ni to the Pt catalyst increases metallic site/acid site ratio. When the ratio of a bifunctional catalyst is less than the optimal value for isomerization, increased metal function of the catalysts prompts the formation of isomers and also inhibits fuel gas formation; examples were shown in the comparison of the yield patterns of C_6 and C_7 reactions catalyzed by Pt(0.26) catalyst and Ni(0.5)–Pt(0.26) catalyst (Tables 1 and 2). However, when there are enough metallic sites to form olefins for feeding all the acid sites, further increased metal function decreases fuel gas formation but concomitantly thwarts the isomerization reaction. As indicated in Tables 1 and 2, both the fuel gas and the isomer yields of C_6 and C_7 catalytic reactions decreased when Ni content was increased from 0.5 to 1.5 wt%.

For C_5 feed, the Ni(0.5)–Pt(0.26) catalyst also exhibits better catalytic performance than the Pt catalyst (Fig. 9). Since the fuel gas formed from C_5 conversion over the test catalyst samples is negligible, the superior catalytic performance of the Ni(0.5)–Pt(0.26) catalyst is due mainly to the higher isomer yields. This result also indicates that the number of metallic sites on the Pt(0.26) catalyst is smaller than the optimal value for C_5 isomerization. The addition of Ni to the Pt catalyst increases metal sites, thereby increasing C_5 isomer formation.

Catalytic Properties of Pt and Ni–Pt Catalysts for Sulfur-Containing Feed

The addition of Ni to the Pt catalyst leads to a decrease in fuel gas formation for feed containing no sulfur. In contrast, for feed containing 500 ppm sulfur, no suppression of fuel gas formation is observed. Instead, more fuel gas is formed, as observed for the Ni(0.5)–Pt(0.26) catalyst (Fig. 10). The details of the chemistry of this abnormally high fuel gas formation remain to be investigated. However, together with the catalytic performance test and TPR results, it suggest a role for Ni–Pt bimetallic interactions.

The thiophene conversion catalyzed by the Pt(0.26) catalyst is slightly higher than that by the Ni(0.5)–Pt(0.26)

catalyst (Fig. 12), and the number of metal sites, which are characterized by CO chemisorption, on the Pt catalyst is smaller than the number on the Ni(0.5)–Pt(0.26) catalyst. If Ni and Pt particles on the Ni(0.5)–Pt(0.26) catalyst are segregated, implying no difference in electronic properties of the Pt particles between the Pt and the Ni–Pt catalysts, we may expect the number of unpoisoned metal sites on the Ni–Pt catalyst to be larger than that on the Pt catalyst and the rate of fuel gas formation to be lower. But the opposite is true of our experimental results. Accordingly, we may conclude that the Pt particles on Ni–Pt catalyst may have electronic properties different from those on the Pt catalyst and are more easily poisoned by H_2S.

Ni–Pt bimetallic interactions may induce electron transfer from Ni to Pt and thus increase the electron density of Pt on the Ni–Pt catalyst. The increase in electron density promotes the adsorption of electrophilic H_2S on the Pt surface (18–21), leading to decreases in the unpoisoned metallic site/acid site ratio (N_M/N_A). As a result, instead of suppressing fuel gas formation by adding Ni to the Pt catalyst, fuel gas formation is promoted when the feed contains 500 ppm sulfur.

The total conversion of C_6 is shown as a function of time on stream in the flow reactor for each of the two catalysts (Fig. 11). The initial activity of the Ni–Pt catalyst is higher than that of the Pt catalyst, whereas the conversion fell more rapidly. The results indicate that the Ni–Pt catalyst underwent a more rapid deactivation than did the Pt catalyst. For a light naphtha isomerization catalyst, the catalyst deactivation is due mostly to the loss of metal function caused by sulfur poisoning and the loss of acid function caused by coke deposition (1–3). Thus, it may be because of Ni–Pt bimetallic interactions that, early in the run, the metal sites on the Ni–Pt catalyst are quickly deactivated by the adsorbed H_2S, leading to a decrease in metal function, thereby enhancing hydrocracking and coke deposition rate; elemental analysis indicated that the residue carbon on the used Pt catalyst is 2.87 wt%, and that on the Ni–Pt catalyst is 3.58 wt%. However, concomitantly with the loss of metal function, the acid sites of the Ni–Pt catalysts are quickly poisoned by the deposited coke, resulting in a quick decrease in total conversion and fuel gas formation.

CONCLUSION

The results of the catalytic test reactions with pure C_5, C_6, and C_7 feed indicate that fuel gas formation is suppressed and the rate of branched isomer formation is elevated by adding a moderate amount of Ni (0.5 wt% Ni of the catalyst) to the mordenite-supported Pt catalyst. Since the N_M/N_A ratio of the Pt catalyst is less than the optimal value for isomerization, the improvement in catalytic performance was thought to be a result of the increase in N_M/N_A ratio. However, with the feed containing 500 ppm sulfur, instead of an improvement in catalytic performance, fuel gas formation was greatly increased by adding Ni to the Pt catalyst. Combined with the results of TPR, TPD, and the catalytic performance test, we speculate that Ni–Pt bimetallic interactions occurred on the Ni–Pt catalyst. Because of these bimetallic interactions, the metal function of the catalyst was quickly lost by sulfur poisoning and fuel gas formation was thus increased.

ACKNOWLEDGMENTS

The support of the National Science Council of the Republic of China (NSC85-2114-E-194-002), National Chung Cheng University, and the Refining & Manufacturing Research Center of Chinese Petroleum Corporation (RMRC) is acknowledged.

REFERENCES

1. Travers, C., "Isomerization of Normal Paraffins." ENSPM-Formation Industrie, 1993.
2. O'Keefe, L. F., Holcombe, T. C., and Sloss, J. R., "Total Isomerization Process (TIP) Innovations," AM-88-48. National Petroleum Refiners Association, 1988.
3. Zarchy, A. S., and Shamshoum, E. S., "Effects of Sulfur on the Performance of Zeolite Isomerization Catalysts." Presented at the Tenth North American Catalysis Society Meeting, San Diego, CA, May 1987.
4. Huang, -W. L., "Study of Paraffins Isomerization Reaction," Annual Research Report, Chinese Petroleum Corporation, 1992.
5. Sinfelt, J. H., "Bimetallic Catalysts, Discoveries, Concepts, and Applications." Wiley, New York, 1983.
6. Thomas, Ch. L., "Catalytic Processes and Proven Catalysts." Academic Press, New York, London, 1970.
7. Ponec, V., *Catal. Rev. Sci. Eng.* **11**, 41 (1975).
8. Sachtler, W. M. H., *Catal. Rev.* **14**, 193 (1976).
9. Bertolini, J. C., Tardi, B., Abon, M., Billy, J., Delichre, P., and Massardier, J., *Surf. Sci.* **135**, 117 (1983).
10. Dominguez, J. M., Vazquez, A., Renouprez, A. J., and Yacaman, M. J., *Surf. Sci.* **75**, 101 (1982).
11. Jones, A., and McNicol, B., "Temperature-Programmed Reduction for Solid Materials Characterization." Marcel Dekker, New York, 1986.
12. Leu, L.-J., Hou, L.-Y., Kang, B.-C., Li, C., Wu, S.-T., and Wu, C. C., *Appl. Catal.* **69**, 49 (1991).
13. Raab, C., Lercher, J. A., Goodwin, J. G., Jr., and Shyu, J. Z., *J. Catal.* **122**, 406 (1990).
14. Augusstine, S. M., and Sachtler, W. M. H., *J. Catal.* **116**, 184 (1989).
15. Mieville, R. L., *J. Catal.* **87**, 437 (1984).
16. Guisnet, M., Alvarez, F., Giannetto, G., and Perot, G., *Catal. Today* **1**, 415 (1987).
17. Glannetto, G. E., Perot, G. E., and Guisnet, M. R., *Ind. Eng. Chem. Prod. Res. Dev.* **27**, 1391 (1986).
18. Figoli, N. S., and L'argentiere, P. C., *Catal. Today* **5**, 403 (1989).
19. Gallezot, P., *Catal. Rev. Sci. Eng.* **20**(1), 121 (1979).
20. Hegedus, L. L., and McCabe, R. B., "Catalyst Poisoning." Marcel Dekker, New York/Basel, 1984.
21. Tri, T. M., Massardier, J., Gallezot, P., and Imelik, B., *in* "Sulfur Resistance of Modified Platinum Y Zeolite" (B. Imelik *et al.*, Eds.). Elsevier, Amsterdam, 1980.